Electron Cyclotron Heating During ECRH-assisted Pre-ionization in a Tokamak

JaeChun Seol 1), B. H. Park 1), S. S. Kim 1), J. Y. Kim 1), Yong-Su Na 2)

1) National Fusion Research Institute, 113 Gwahangno, Yuseong-Gu, DaeJeon 305-333, Korea
2) Department of Nuclear Engineering, Seoul National University, 599 Gwanangno, Gwanak-gu, Seoul, 151-744, Korea

E-mail contact of main author: jseol@nfri.re.kr

Abstract In this research, we investigate ECRH for low-energy electrons analytically and numerically, which is applicable to ECRH-assisted plasma start-up in a tokamak. From the previous experimental studies, it is well-known that the first harmonic ECRH is more effective than the second harmonic ECRH. In this work, we developed an analytic model of ECRH in the start-up process and present comparisons of the efficiency between the first harmonic and the second harmonic. It is found that electrons gain a large energy from the waves at first harmonic resonance up to several hundred eV. However, electrons gain a large energy from the waves only up to ~10 eV and energy-gain starts decreasing afterward at second harmonic resonance. When seed electrons are heated from the room temperature to far away above the ionization energy, seed electrons can bring about an avalanche of electrons. Thus, pre-ionization with the second harmonic can be delayed since electrons need more time to be heated up to the breakdown temperature due to the slow heating speed compared to the first harmonic ECRH.

1. Introduction

Electron cyclotron resonance heating (ECRH)-assisted plasma breakdown has been proposed in new tokamaks such as KSTAR [1], JT-60SA [2], and ITER [3] since the loop voltage is limited due to thick vacuum liners and superconducting poloidal field coils. An in-vessel toroidal electric field, E_T, available for plasma start-up in ITER will be limited to 0.3 V/m or less. Thus, assist of plasma breakdown by ECRH pre-ionization is needed in ITER-like tokamaks. Fundamental ECRH-assisted breakdown has been investigated in many tokamaks [4, 5, 6, 7, 8]. Second harmonic ECRH breakdown was also robust in DIII-D [9] and KSTAR [10]. In the KSTAR tokamak, ECRH pre-ionization has been performed for the first time as a fully superconducting tokamak. However, first harmonic ECRH start-up has been observed to be more effective than second harmonic ECRH start-up in the previous experimental studies. Diagnostic signals that indicate occurrence of pre-ionization were detected with the time delay from ECRH-onset for the second harmonic ECRH start-up, while prompt with the first harmonic ECRH. Generally, the efficiency of second harmonic X-mode heating is considered as comparable with that of fundamental O-mode heating. However, ECRH breakdown is delayed with the second harmonic X-mode heating while ECRH breakdown occurs immediately with the first harmonic O-mode.

Recently, a collisionless nonlinear cyclotron heating model was developed with passing particles and the realistic wave beam profile [11]. Nonlinear cyclotron harmonic absorption occurs at first, second and third harmonic resonances when particles pass the resonance zone slowly [11]. In ref. [11], the second harmonic ECRH is described in detail analytically and numerically. In the present work, we investigate the first harmonic ECRH as a succeeding study of Ref. [11] and to present a comparison with the second harmonic ECRH while ref. [11] focused on the second harmonic ECRH.

A review of nonlinear cyclotron absorption is given in Sec. 1. In Sec. 2, we identify key parameters of the first harmonic nonlinear cyclotron absorption and present a comparison between the first harmonic and the second harmonic nonlinear ECRH. Finally, a summary and a discussion of the results are presented in Sec. 3.

2. Analytic Description

Analytic descriptions of collisionless nonlinear cyclotron absorption have been introduced previously [11]. In this paper, we briefly show a heuristic derivation procedure introduced in Ref. [11].

To demonstrate interactions between waves and particles, we solve the Lorentz equation for electrons:

$$\frac{d(\gamma m_0 \vec{v})}{dt} = -e(\vec{v} \times \vec{B} + \vec{E}) \tag{1}$$

where

$$\gamma = \left(1 - \frac{\vec{v}\cdot\vec{v}}{c^2}\right)^{-1/2}$$

and c, $\vec{E}$, m_0 and $\vec{B}$ are the light speed, the electric field, the electron rest mass, and the magnetic field respectively. The electric field of the microwaves is assumed to be left circularly polarized for cyclotron resonance with electrons:

$$\vec{E} = E_x \hat{x} \sin(kx - \omega t) + E_y \hat{y} \cos(kx - \omega t) \tag{2}$$

and $E_x \equiv E_y \equiv E_0/2$ where k, ω and E_0 are the wave number, the wave frequency and the electric field strength respectively. A rigorous analysis must consider the effects of dispersed waves. Unfortunately, this will make the analysis extremely complicated. Also, it is quite likely that the electric field of dispersed waves is fairly small compared to the field illuminated directly on the resonance layer. We also assume that the magnetic field strength is constant in the resonance zone due to its relatively short width compared to the ripple period.

The phase factor is expressed as

$$\psi = \int_{t_0}^{t} dt' \Omega_{ce}(t') + \psi_0$$

where the electron cyclotron frequency, $\Omega_{ce}(t) = eB/\gamma m_0$ and ψ_0 is the initial phase of the particle. For the microwaves, we can assume that $k\rho_L \ll 1$. When $k\rho_L \ll 1$, $J_n(k\rho_L) \approx (k\rho_L)^n/2^n n!$. Here, we define new variables, $\Psi \equiv n\psi - \omega t$ and $\Gamma \equiv \gamma - 1$. At the cyclotron resonance, Ψ remains constant in a nonrelativistic case. As the relativistic effect is considered on the cyclotron frequency, Ψ varies with time. The other newly-defined variable Γ is nothing but the ratio of the kinetic energy of electrons to the rest mass energy $m_0 c^2$. With these variables and another dimensionless variable $\varepsilon \equiv eE_0/m_0 c\omega$, Eqs. (**??**)-(**??**) become

$$\begin{aligned} \frac{d\Psi}{dt} &= -\Gamma\omega - \frac{\varepsilon\omega}{(n-1)!}\left(\frac{n}{2}\right)^{n-1} 2^{\frac{n}{2}-1}\frac{n}{2} \\ &\quad \times \Gamma^{n/2-1}(-1)^{n/2}\cos\Psi \qquad n = even \qquad (3) \\ &= -\Gamma\omega + \frac{\varepsilon\omega}{(n-1)!}\left(\frac{n}{2}\right)^{n-1} 2^{\frac{n}{2}-1}\frac{n}{2} \\ &\quad \times \Gamma^{n/2-1}(-1)^{(n-1)/2}\sin\Psi \qquad n = odd, \qquad (4) \end{aligned}$$

and

$$\frac{d\Gamma}{dt} = -\frac{\varepsilon\omega}{(n-1)!}\left(\frac{n}{2}\right)^{n-1} 2^{\frac{n}{2}-1} \times\Gamma^{n/2}(-1)^{n/2}\sin\Psi \qquad n = even \tag{5}$$

$$= -\frac{\varepsilon\omega}{(n-1)!}\left(\frac{n}{2}\right)^{n-1} 2^{\frac{n}{2}-1} \times\Gamma^{n/2}(-1)^{(n-1)/2}\cos\Psi \qquad n = odd. \tag{6}$$

Equations (3)-(6) can be combined into

$$\Gamma^2 - 2\varepsilon\alpha\Gamma^{n/2}\cos\Psi = C_1 \qquad n = even \tag{7}$$

$$\Gamma^2 - 2\varepsilon\alpha\Gamma^{n/2}\cos\left(\Psi+\frac{\pi}{2}\right) = C_2 \qquad n = odd, \tag{8}$$

where C_1 and C_2 are constant,

$$\alpha \equiv -\frac{g}{(n-1)!}\left(\frac{n}{2}\right)^{n-1} 2^{\frac{n}{2}-1}$$

and $g = (-1)^{n/2}$ when n is an even integer and $g = (-1)^{(n-1)/2}$ when n is an odd integer.

3. Comparison between 1st and 2nd harmonic ECRH

Nonlinear collisionless cyclotron absorption at the second harmonic resonance was investigated analytically and numerically in the previous study[11]. In this section, we investigate nonlinear cyclotron absorption at the first harmonic resonance and we also study the second harmonic ECRH on low-energy electrons, which is relevant to pre-ionization process in a tokamak start-up phase. We then compare first and second harmonic ECRH.

The phase difference and the particles energy at the first harmonic resonance can be obtained by solving

$$\frac{d\Psi}{dt} = -\Gamma\omega + \frac{\varepsilon\omega}{2\sqrt{2}}\Gamma^{-1/2}\sin\Psi \tag{9}$$

$$\frac{d\Gamma}{dt} = -\frac{\varepsilon\omega}{\sqrt{2}}\Gamma^{1/2}\cos\Psi. \tag{10}$$

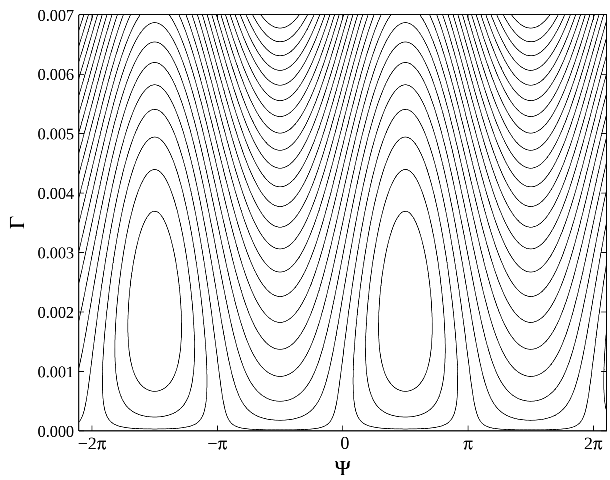

FIG. 1. Γ vs Ψ at the first harmonic cyclotron resonance. $\varepsilon = 2.67\times10^{-4}$.

Equations (9) and (10) can be combined into

$$\Gamma^2 - \sqrt{2}\Gamma^{1/2}\varepsilon \sin\Psi = C, \tag{11}$$

where C is constant. Contours of Eq. (11) indicates that Γ varies periodically as shown in Figure . Figure also shows that closed contours, so called "trapped mode", exist and they are approximately concentric as expected in Ref. [11]. For a trapped mode, $\cos\Psi = 0$ and $\sin\Psi = 1$ at the extreme values of Γ. Thus, the axis of the first harmonic Γ-oscillation estimated from Eq. (11) to be $\sim \varepsilon^{2/3}/2$ while the axis of the second harmonic Γ-oscillation is $\sim \varepsilon$. Since $\varepsilon \ll 1$, the energy oscillation of the first harmonic ECRH occurs with much higher energy value than that of the second harmonic ECRH. Table shows the comparison of the axis of Γ-oscillation between the first and the second harmonic ECRH. In the reality, the wave beam intensity varies spatially across the wave beam. Due to this spatial inhomogeneity, the axis of energy-oscillation varies as the electrons pass the wave beam according to the wave electric field strength (Figure). In this study, we assume that the wave beam intensity has a Gaussian profile.

Here, we estimate Γ approximately with focusing only on determination of the oscillation frequency. From Eqs. (10) and (11), we obtain

$$\frac{d\Gamma}{\left(-\Gamma^4 + 2C\Gamma^2 + 2\Gamma\varepsilon^2 - C^2\right)^{1/2}} = -\frac{\omega}{2}dt. \tag{12}$$

Equation (12) can be solved analytically in terms of the Weierstrass elliptic function [12]:

$$\Gamma = \Gamma_0 + \frac{-\Gamma_0^3 + C\Gamma_0 + \varepsilon^2/2}{\wp\left(-\frac{\omega}{2}(t-t_0); g_2, g_3\right)} \tag{13}$$

where $\wp$ is the Weierstrass function and the invariants are given by $g_2 = 13C^2$ and $g_3 = 2C^3 + 4\varepsilon^4$. Here, Γ_0 is any root of $-\Gamma^4 + 2C\Gamma^2 + 2\Gamma\varepsilon^2 - C^2 = 0$ and $\Gamma(t_0) = \Gamma_0$. When the particle's energy oscillates very near the axis of oscillation, $\Gamma \sim \varepsilon^{2/3}/2$. Since $g_2^3 - 27g_3^2 > 0$ in this case, Eq. (13) can be rewritten as

$$\Gamma \approx \Gamma_0 + \frac{-\Gamma_0^3 + C\Gamma_0 + \varepsilon^2/2}{-1.02854\varepsilon^{4/3} + 2.55848\varepsilon^{4/3}/\mathrm{sn}^2\left[-0.71262\omega\varepsilon^{2/3}(t-t_0); 0.454\right]} \tag{14}$$

where sn is the Jacobi elliptic function.

Since the Jacobi elliptic function in Eq. (14) has a period of $4\mathrm{K}(0.454)$, the energy-oscillation frequency at the first harmonic can be estimatied as $1.23153 f_{rf}\varepsilon^{2/3}$ where f_{rf} is the ECRH microwave frequency. Recalling $\varepsilon \ll 1$, the oscillation frequency of the first harmonic resonance is larger than the second harmonic oscillation frequency, $f_{rf}\varepsilon$. The comparison of the oscillation axis and the frequency between the first and the second harmonic is given in Table .

As particles pass the wave beam, particles obtain net collisionless heating when wave-particle interaction time is larger than the energy-oscillation period. This means that the first harmonic ECRH is more favorable for nonlinear collisionless heating than the second harmonic since the energy-oscillation time period of the first harmonic is much shorter than that of the second harmonic. For the first harmonic ECRH, nonlinear energy-oscillation occurs when

$$\begin{aligned} T_{oscillation} &\simeq \frac{1}{1.23\varepsilon^{2/3} f_{rf}} < \tau_{passing} = \frac{L_b}{v_{||}} \\ v_{||} &< 1.23 L_b \varepsilon^{2/3} f_{rf} \end{aligned} \tag{15}$$

where $T_{oscillation}$, $\tau_{passing}$, $v_{||}$, and L_b are the nonlinear energy-oscillation period, time needed for particles to pass the wave beam, parallel speed of particle and the wave beam width, respectively. For the second harmonic ECRH, the condition

$$v_{||} < L_b \varepsilon f_{rf} \tag{16}$$

needs to be satisfied to get the nonlinear energy-oscillation. In the start-up process in a tokamak, seed electrons are heated from the room temperature. Since electrons stay in the resonance region relatively longer, nonlinear energy-oscillations can occur easily in the start-up process. For the parameters in KSTAR: $L_b = 8.2$ cm, f_{rf}=84 GHz, and $\varepsilon = 2.67 \times 10^{-4}$. With the parameters of KSTAR, the maximum parallel speed for nonlinear energy-oscillation and consequently large energy kick at the second harmonic resonance is obtained from Eq. (16); $W_{in} <\sim 9.1$ eV where W_{in} is the energy of the particle at the entrance of the wave beam. For the first harmonic, we obtain $W_{in} <\sim 1035$ eV from the Eq. (15). Thus, a large energy gain per passage occurs up to much larger value of W_{in} with the first harmonic ECRH than with the second harmonic. Due to this nonlinear energy-oscillation, the first harmonic ECRH is much more effective than the second harmonic for low-temperature electron heating, which is relevant to the pre-ionization in a tokamak. The pre-ionization occurred promptly in the previous experimental studies since electrons are heated to several hundred eV quickly through the nonlinear energy absorption with the first harmonic. With the second harmonic, electrons are heated quickly only up to $\sim$10 eV and heated slowly through stochastic heating until they reach far above the ionization temperature and finally bring about an avalanche of electrons. Consequently, a time-delay of plasma breakdown can occur in the start-up process in a tokamak with the second harmonic.

Energy increase per passage through the wave beam is calculated numerically with respect to the initial energy to compare with the analytical results. For the numerical calculation in this study, we use the parameters of the KSTAR tokamak. Figure (a) shows that the energy gain stays large until the particle's energy at the entrance of the wave beam reaches $\sim$600 eV and decreases thereafter with the first harmonic. On the other hand, Figs (b) and (c) show that energy gain starts decreasing after $W_{in} \sim$10 eV with the second harmonic. As shown, the numerical calculations approximately agree with the analytic estimations presented above based on the model developed in this research.

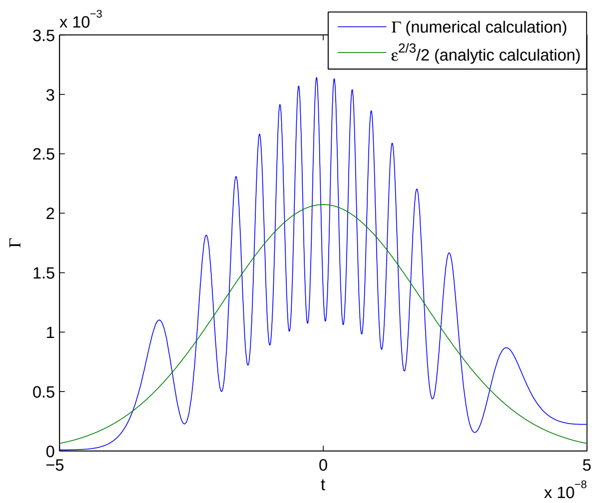

FIG. 2. The axis of oscillation at the first harmonic resonance varies with $\varepsilon^{2/3}/2$. The wave is assumed to have a Gaussian beam profile. The particles travels from t=-∞ to t=∞ and pass the center of the beam at t=0.

TABLE I: THE AXIS OF OSCILLATION AND THE FREQUENCY OF NONLINEAR ENERGY-OSCILLATION OF FIRST AND SECOND HARMONIC X-MODE ECRH FOR A TRAPPED-MODE IN THE START-UP PROCESS.

	1st harmonic	2nd harmonic
Axis of oscillation	$\varepsilon^{2/3}/2$	ε
energy-oscillation frequency	$1.23\varepsilon^{2/3}f$	εf

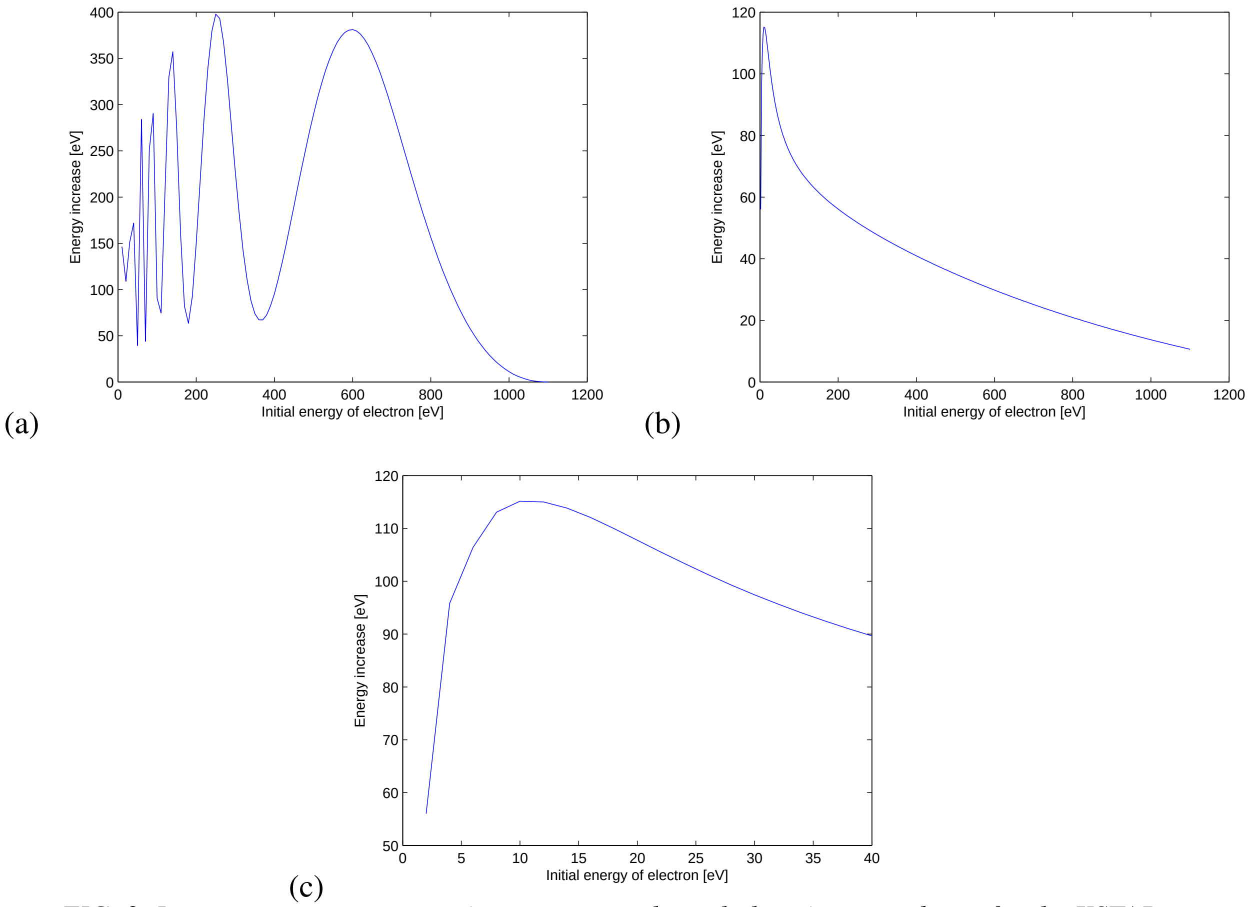

FIG. 3. Input energy vs. energy gain per passage through the microwave beam for the KSTAR parameters at (a) the first and (b) the second harmonic resonances. (c) Energy gain at the second harmonic resonance is calculated for electrons of the initial energy around 10 eV.

4. Summary

In this research, we investigated the nonlinear cyclotron resonance heating focusing on the first harmonic resonance based on the previous study [11]. We identified the key parameters of the nonlinear first harmonic ECRH. We found that the axis of nonlinear energy-oscillation for the first harmonic is about one order of magnitude higher than that of the second harmonic. We also found that energy-oscillation frequency of the first harmonic is larger than the second harmonic also by about one order of magnitude. Consequently, we can conclude that nonlinear energy-oscillation occurs more easily with the first harmonic ECRH than the second harmonic.

We calculated the energy increase of low-energy electrons per pass through the wave beam using the analytical model developed in this study. It was found that electrons gain a large energy from the waves through a single passage at the first harmonic resonance due to nonlinear energy oscillation until electron's energy at the entrance of the wave beam is around several hundred eV, which is determined by Eq. (15). However, energy gain of electrons decreases as electron's energy at the entrance increases when the entrance particle energy is larger than the maximum value determined by Eq. (15). Thus, ECRH can heat up low-energy electrons to several hundred eV rapidly with the first harmonic resonance. In the pre-ionization process in a tokamak, electrons are heated from the room temperature. Therefore electrons can be heated to far above the ionization energy very rapidly and bring about an avalanche of electrons, i.e. pre-ionization, immediately with the first harmonic ECRH in the tokamak startup phase according to the analytical model developed in this study.

However, energy gain of electron is large only when the entrance electron energy is smaller than $\sim$ 10 eV which is determined by Eq. (16) and starts decreasing as electron's energy increases to the larger value than the maximum value (10 eV with the KSTAR parameters) at second harmonic resonance. The second harmonic ECRH heats up electrons to $\sim$10 eV quickly and then slow down the heating speed. In the pre-ionization process in a tokamak, electrons are heated from the room temperature to $\sim$10 eV quickly which does not reach the ionization energy and are heated slowly until electron's energy reaches the energy large enough to bring about an avalanche of electrons for the second harmonic. Thus, pre-ionization with the second harmonic ECRH is delayed due to low nonlinear ECRH efficiency of the second harmonic ECRH, while there is no such delay with the first harmonic ECRH, as observed in the previous experimental studies.

Numerical calculation was also performed to compare with the analytic calculation. Numerical calculation was consistent with the analytic estimation. Numerical calculation clearly showed that the first harmonic nonlinear ECRH is more effective than the second harmonic ECRH.

References

[1] G. S. Lee et al. The KSTAR project: An advanced steady state superconducting tokamak experiment. *Nucl. Fusion*, 40:575–582, 2000.

[2] T. Fujita et al. Design optimization for plasma performance and assessment of operation regimes in JT-60SA. *Nucl. Fusion*, 47:1512–1523, 2007.

[3] Y. Gribov, D. Humphreys, K. Kajiwara, E.A. Lazarus, J.B. Lister, T. Ozeki, A. Portone, M. Shimada, A. C. C. Sips, and J. C. Wesley. Progress in the ITER Physics Basis, Chapter 8: Plasma operation and control. *Nucl. Fusion*, 47:S385, 2007.

[4] K. Kajiwara, Y. Ikeda, M. Seki, S. Moriyama, T. Oikawa, T. Fujii, and the JT-60 Team. Electron cyclotron heating assisted startup in JT-60U. *Nucl. Fusion*, 45:694–705, 2005.

[5] D. R. Whaley, T. P. Goodman, A. Pochelon, R. Behn, A. Cardinali, B. P. Duval, B. Joye, and M. Q. Tran. X- and O-mode electron cyclotron heating breakdown and startup in TCA. *Nucl. Fusion*, 32:757–771, 1992.

[6] S. Tanaka, K. Hanada, T. Minami, S. Ide, M. Iida, H. Tanaka, T. Maekawa, and Y. Terumichi. Initiation of plasma current with the assistance of electron cyclotron waves in the WT-3 tokamak. *Nucl. Fusion*, 33:505–513, 1993.

[7] B. Lloyd, G. L. Jackson, T. S. Taylor, E. A. Lazarus, T. C. Luce, and R. Prater. Low voltage ohmic and electron cyclotron heating assisted startup in DIII-D. *Nucl. Fusion*, 31:2031–2053, 1991.

[8] A. G. Kulchar, O. C. Eldridge, A. C. England, C. E. Bush, P. H. Edmonds, G. G. Kelley, C. M. Loring, Y-K. M. Peng, J. B. Wilgen, and S. K. Borowski. Preionization and start-up in the ISX-B tokamak using electron cyclotron heating at 28 GHz. *Phys. Fluids*, 27:1869, 1984.

[9] G. L. Jackson, J. S. deGrassie, C. P. Moeller, and R. Prater. Second harmonic electron cyclotron pre-ionization in the DIII-D tokamak. *Nucl. Fusion*, 47:257–263, 2007.

[10] Y.S. Bae, J.H. Jeong, S.I. Park, M. Joung, J.H. Kim, S.H. Hahn, S.W. Yoon, H.L. Yang, W.C. Kim, Y.K. Oh, A.C. England, W. Namkung, M.H. Cho, G.L. Jackson, J.S. Bak, and the KSTAR team. Ech pre-ionization and assisted startup in the fully superconducting kstar tokamak using second harmonic. *Nuclear Fusion*, 49(2):022001, 2009.

[11] JaeChun Seol, C. C. Hegna, and J. D. Callen. Nonlinear cyclotron harmonic absorption. *Phys. Plasmas*, 16:052512, 2009.

[12] E. T. Whittaker and G. N. Watson. *A Course of Modern Analysis*. Cambridge University Press, The Pitt Building, Trumpington Street, Cambridge, United Kingdon, 1996.